International Journal of Medical, Medicine and Health Sciences
ISSN: 2517-9969
Vol:4, No:2, 2010

Flow Regime Characterization in a Diseased Artery Model

Anis S. Shuib, Peter R. Hoskins and William J. Easson

***Abstract*—**Cardiovascular disease mostly in the form of atherosclerosis is responsible for 30% of all world deaths amounting to 17 million people per year. Atherosclerosis is due to the formation of plaque. The fatty plaque may be at risk of rupture, leading typically to stroke and heart attack. The plaque is usually associated with a high degree of lumen reduction, called a stenosis. The initiation and progression of the disease is strongly linked to the hemodynamic environment near the vessel wall. The aim of this study is to validate the flow of blood mimic through an arterial stenosis model with computational fluid dynamics (CFD) package. In experiment, an axisymmetric model constructed consists of contraction and expansion region that follow a mathematical form of cosine function. A 30% diameter reduction was used in this study. Particle image velocimetry (PIV) was used to characterize the flow. The fluid consists of rigid spherical particles suspended in water-glycerol-NaCl mixture. The particles with 20 μm diameter were selected to follow the flow of fluid. The flow at *Re*=155, 270 and 390 were investigated. The experimental result is compared with FLUENT simulated flow that account for viscous laminar flow model. The results suggest that laminar flow model was sufficient to predict flow velocity at the inlet but the velocity at stenosis throat at *Re* =390 was overestimated. Hence, a transition to turbulent regime might have been developed at throat region as the flow rate increases.

***Keywords*—**Atherosclerosis; Particle-laden flow; Particle image velocimetry; Stenosis artery

I. INTRODUCTION

CARDIOVASCULAR diseases, principally atherosclerosis, are responsible for 30% of world deaths. World Health Organization (WHO) reported coronary heart disease, stroke and other cerebrovascular diseases are the leading causes of global death. Cardiovascular diseases are associated with abnormal blood flow patterns that can cause heart attacks and stroke. Atherosclerosis is associated with vessel narrowing due to accumulation of foam cells engorged with low-density lipoprotein cholesterol causing localized constrictions called 'stenoses'. Stenoses build-up prevents a sufficient supply of oxygen and nutrition to the body.

A. S. Shuib is with the Universiti Teknologi Petronas, Malaysia (corresponding author to provide phone: 605-368-7574; fax: 605-365-6176; e-mail: anisuha@petronas.com.my).

P. R. Hoskins, is with the Department of Medical Physics, University of Edinburgh,UK (e-mail: p.hoskins@edinburgh.ed.ac.uk).

W. J. Easson is with Department of Mechanical Engineering, University of Melbourne, Australia on sabbatical leave from Institute for Materials and Processes, University of Edinburgh, UK (e-mail: weasson@unimelb.edu.au).

The main method used to characterize the flow field in blood vessels are in vivo experimentation, and physical and computational modeling. Computational fluid dynamics (CFD) is preferred because of relative ease of reproducing vascular geometry, varying boundary conditions and the comprehensiveness and convenient format of the results. CFD methods based on solving two- or three-dimensional equations by breaking up a complex geometry into many smaller but simpler shapes. The result is a detailed representation of the velocity and pressure fields. Engineering flow measurement technique such as laser doppler velocimetry (LDV) and particle image velocimetry (PIV) continue to play a key role in applications. CFD remains relative immature where flow instabilities and/or turbulence may occur [1, 2]. Experimental models has been accepted as the gold standard for numerical validation [3].

Flow in cardiovascular system is generally of a low Reynolds number and laminar. However, in the presence of stenoses, transition and turbulence can be generated. In arterial system, abundance of CFD flow simulations that employed laminar [4, 5]or turbulence model [6, 7] have been put forward but lacking of experimental validation [8, 9].

The aim of this paper is to physically measure the flow velocity of a blood analog suspension in a stenosis artery model. The flow conditions are then simulated using CFD technique with laminar and simple turbulent flow model. The simulated results were compared with experimental data.

II. EXPERIMENTAL SYSTEM AND TECHNIQUES

A. Stenosis Artery Model

An axisymmetric stenosis model is manufactured from silicone rubber by casting around a pair of rods whose ends are shaped. The two brass rods with a diameter of 8mm are machined into a mathematical shape consisting of 2 quarter cosines in a controlled lathe. The two ends of the rods are slotted together and held in a rectangular container. Silicone elastomer (Sylgard 184, Dow Corning) is poured in the container and allowed to stand for 24 hours. The rods are pulled out from the sides of the container carefully. The resultant shape of the stenosis phantom with 30% diameter reduction is shown in Fig. 1. The inlet diameter of the tube, *D* is 8mm and the entrance length immediately before and after

the stenosis are 190mm and 94mm respectively. The axial length in the stenosis region is 2*D*.

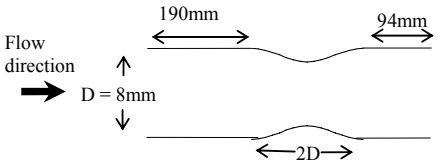

Fig. 1 A schematic stenosis geometry with 30% diameter reduction (length not to scale)

The flow of the fluid is steady and driven by a peristaltic pump (Masterflex L/S, Cole-Parmer Instrument) through a pulse dampener before entering the stenosis artery model. The flow rate is varied between inlet fluid Reynolds number, *Re* of 155, 270 and 390. Reynolds number is defined as

$$Re = \frac{\rho D v}{\mu} \quad (1)$$

where ρ denotes the density of the fluid, D is the inlet diameter of the tube, v_{is} the mean inlet velocity of the fluid, and μ is the viscosity of the fluid.

B. Flow Measurement

A particle image velocimetry (PIV) system (Dantec Dynamics Ltd., UK) is used to acquire the images of particle distribution in the flow. From the images recorded, the velocity vector is calculated. The PIV set-up consisted of an Nd:YaG pulsed laser (Newwave Solo 200XT) of wavelength 532nm with repetition rate between 8 to 21Hz, a high speed digital camera (Kodak Megaplus ES 1.0) with maximum of 15 frame per second for double frame mode and a computer interface (FlowMap, Dantec Dynamics, UK). The set-up is shown in Fig. 3. With flow illuminated, the camera acquired images of the flow field. The area of interest is at the recirculation region where the flow separation occurred

C. Fluid Suspension

The fluid consists of particles suspended in liquid. The liquid is formulated to have a refractive index matched to the flow phantom material. The compositions of the liquid by weight are glycerol 37.1%, water 47.9% and NaCl 15.0%. The refractive index of both liquid and the silicone model is 1.41. The viscosity of the liquid solution is 6.23±0.01mPas and the density is 1080kg/m^3. The particles chosen are spherical rigid particles made from polyamide material (Orgasol, Elf-atochem, France). The density of the particle is 1030kg/m^3 hence it is assumed neutrally buoyant. The properties are summarized in Table I and Table II. The particles sizes are 20±2μm diameter. The weight of particles is measured and then mixed with glycerol-water-NaCl solution. Particles concentrations, ϕ_m of 0.14% by weight were prepared. The particle suspension is stirred for 30 minutes and filtered to remove remaining clumps. The distribution of particles in the solution was observed under microscope (Zeiss, Germany) to ensure particles are not aggregate and moved as a single particle in the fluid. The temperature is kept constant at 20˚C.

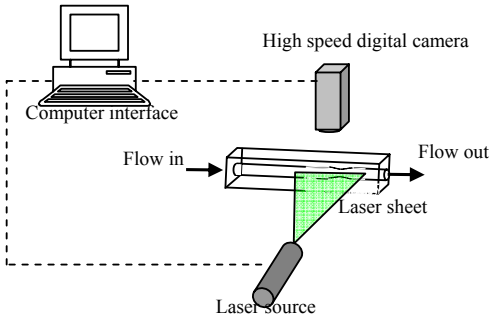

Fig. 2 Schematic representation of the PIV setup

TABLE I
FLUID PROPERTIES

Compositions (w/w%)	Viscosity,μ	Density,ρ
Glycerol = 37.1 Water = 47.9 NaCl = 15.0	6.23 ± 0.01 mPas	1080 kg/m^3

TABLE II
PARTICLES PROPERTIES

Material	Polyamide (Orgasol)
Shape	Rigid, roughly sphere
Diameter, d_p	20±2 μm
Density,ρ_p	1030 kg/m^3
Concentration,ϕ_m	0.14 % (weight)

III. COMPUTATIONAL FLUID DYNAMICS (CFD) SIMULATIONS

A 2D geometry of the stenosis artery model was constructed using Gambit 2.0.4 with quadrilateral grids. There are 108800 quadrilateral cells for the whole geometry. The simulations were carried out using FLUENT 6.3.26. Two solver has been selected; laminar model and turbulent model.

In laminar model, FLUENT solves conservation equations for mass and momentum. For turbulent models, additional transport equations are solved. In a continuous phase of a steady state system, the continuity equations can be written as

$$\frac{\partial \rho}{\partial t} + \nabla \cdot (\rho \vec{v}) = 0 \quad (2)$$

where v is the resultant velocity and ρ is the density of the fluid. Momentum conservation equation is given by

$$\frac{\partial}{\partial t}(\rho\vec{v})+\nabla\cdot(\rho\vec{v}\vec{v})=-\nabla p+\nabla\cdot\left(\bar{\bar{\tau}}\right)+\rho\vec{g}+\vec{F} \quad (3)$$

where p is the static pressure, τ is the stress tensor and F is

$$\bar{\bar{\tau}}=\mu\left[\left(\nabla\vec{v}+\nabla\vec{v}^{T}\right)-\frac{2}{3}\nabla\cdot\vec{v}I\right] \quad (4)$$

the gravitational forces and external body forces. The stress tensor τ is described as

where μ is the viscosity, I is the unit tensor and T is the stress vector.

In considering turbulence nature of flow, Reynolds Stress model which based on Reynolds averaged Navier-Stokes (RANS) approach was chosen. The velocity component u_i is defined as

$$u_i=\bar{u}_i+u' \quad (5)$$

where $\bar{u}_i$ and u_i' are the mean and fluctuating velocity component respectively. i = 1,2,3,…

Hence, for turbulence the Reynolds-averaged momentum equations are as follows

$$\frac{\partial}{\partial t}(\rho u_i)+\frac{\partial}{\partial x_j}(\rho u_i u_j)=-\frac{\partial p}{\partial x_i}+\frac{\partial}{\partial x_j}\left[\mu\left(\frac{\partial u_i}{\partial x_j}+\frac{\partial u_j}{\partial x_i}-\frac{2}{3}\delta_{ij}\frac{\partial u_l}{x_l}\right)\right]+\frac{\partial}{\partial x_j}R_{ij} \quad (6)$$

where R_{ij} is the Reynolds stress tensor. It's an additional unknown introduced by the averaging procedure.

$$R_{ij}=-\rho\,\overline{u_i'u_j'} \quad (7)$$

In order to close the system of governing equations, another model is introduced called Reynolds-Stress model. The equation is given by

$$\frac{\partial}{\partial t}\left(\rho\,\overline{u_i'u_j'}\right)+\frac{\partial}{\partial x_k}\left(\rho\,u_k\overline{u_i'u_j'}\right)=P_{ij}+F_{ij}+D_{ij}^{T}+\Phi_{ij}-\varepsilon_{ij} \quad (8)$$

where P_{ij} is the stress production, F_{ij} is the system rotation production, D_{ij}^{T} is the turbulent diffusion, Φ_{ij} is the pressure strain and ε_{ij} is the dissipation.

The above equations were solved for two dimensional Newtonian flow in an axisymmetric stenosis geometry.

IV. Results and Discussions

The flow field at Re=270 measured by particle image velocimetry is shown in Fig. 3. Fig. 3a. indicates the location of the measured field of the stenosis which represented by the rectangular box. Two locations were measured with one at the inlet of the stenosis and the other at the throat of the stenosis denominated by A and B respectively. The inlet velocity profile starts at 111cm from the flow entrance and the stenosis throat starts at 201mm from flow inlet. The dimensions were not to scale.

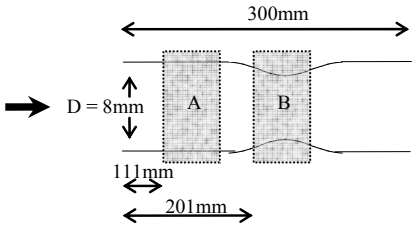

a. Measurement location (not to scale)

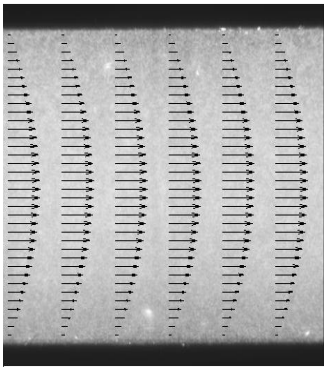

b. Vector field at location A (inlet of stenosis)

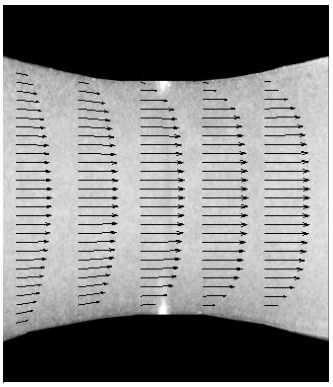

c. Vector field at location B (throat)

Fig. 3 Measured velocity vector overlapped on flow field image at the inlet and throat of stenosis

The resultant velocity vector of the flow is overlapped on the image as shown in Fig. 3b and 3c.The enlarged images fields are shown below with the actual frame size of 8.2x8.2mm. 1mm length of vector arrow is equivalent to 0.4m/s. The flow before entering the stenosis was fully developed following parabolic poiseuille equation.

$$v = v_{max}(1 - r^2/R^2) \quad (9)$$

where v_{max} is the maximum velocity, r is the local radial position and R is the radius of the flow section. Based on conservation of mass and energy, the pressure fell along the tube, but when entering the stenosis throat the pressure dropped at a faster rate, hence, the velocity increases.

Fig. 4 shows the velocity profile of stenosis inlet at *Re*=155, *Re*=270 and *Re*=390 at *x*=116mm. The experimental results and computer simulation data (Laminar model) are plotted together. The results were fully developed according to poiseuille equation with maximum velocity at central radial axis, v_{max} of 0.20m/s, 0.36m/s and 0.52m/s respectively.

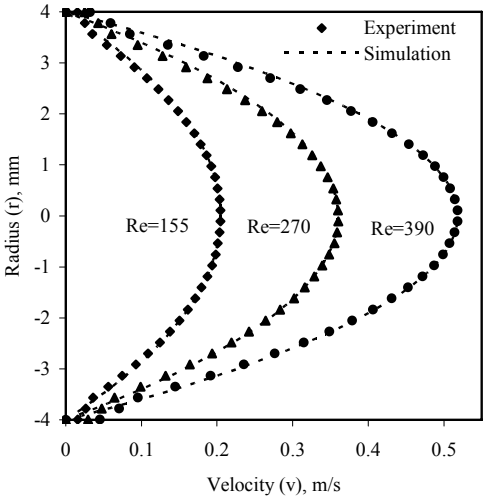

Fig. 4 Measured and simulated inlet velocity profile

Simulation results for laminar and turbulence model at stenosis throat is plotted together with the experimental results in Fig 5. At *Re*=155, the simulated results assuming laminar flow predict the measured velocity correctly, however the turbulent model underestimates the velocity in the core region with blunted face. Similarly, at *Re*=270 the measured velocity profile having similar pattern predicted by simulated laminar model. For *Re*=390 the velocity profile for laminar model overestimated the measured velocity. The experimental velocity at the core region was less up to 8% difference. The maximum velocity in turbulence model is closer to the experimental results. However, the measured velocity profile remained parabolic.

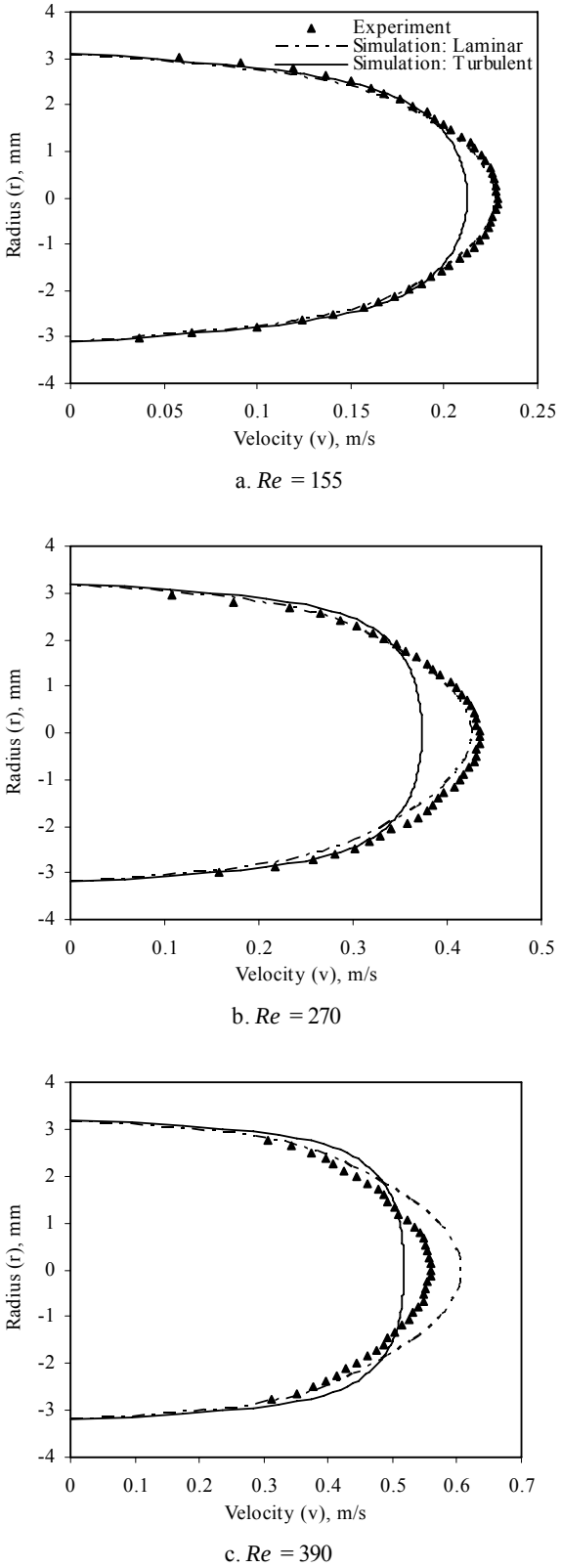

Fig. 5 Measured and simulated velocity at the throat of the stenosis

V. Conclusion

This study demonstrated the importance of choosing the right solver to analyze CFD generated results. In laminar model, FLUENT solves conservation equations for mass and momentum. For turbulent models, additional transport equations are solved. At low Re, laminar model were sufficient to describe the flow at the stenosis throat. However, as the Re increases, neither laminar nor RANS turbulence model estimates the experimental results appropriately. Averaging method does not resolved turbulent vortex structure predicted at stenosis throat region.

References

[1] C. A. Taylor, and M. T. Draney, "Experimental and computational methods in cardiovascular fluid mechanics," *Annual Review Of Fluid Mechanics,* vol. 36, pp. 197-231, 2004.

[2] D. A. Steinman, and C. A. Taylor, "Flow imaging and computing: Large artery hemodynamics," *Annals Of Biomedical Engineering,* vol. 33, no. 12, pp. 1704-1709, 2005.

[3] M. H. Friedman, and D. P. Giddens, "Blood flow in major blood vessels-modeling and experiments." pp. 1710-1713.

[4] B. Y. Liu, "The influences of stenosis on the downstream flow pattern in curved arteries," *Medical Engineering & Physics,* vol. 29, no. 8, pp. 868-876, Oct, 2007.

[5] V. Deplano, and M. Siouffi, "Experimental and numerical study of pulsatile flows through stenosis: Wall shear stress analysis," *Journal Of Biomechanics,* vol. 32, no. 10, pp. 1081-1090, Oct, 1999.

[6] G. C. Kagadis, E. D. Skouras, G. C. Bourantas *et al.*, "Computational representation and hemodynamic characterization of in vivo acquired severe stenotic renal artery geometries using turbulence modeling," *Medical Engineering & Physics,* vol. 30, no. 5, pp. 647-660, Jun, 2008.

[7] L. Grinberg, A. Yakhot, and G. E. Karniadakis, "Analyzing Transient Turbulence in a Stenosed Carotid Artery by Proper Orthogonal Decomposition," *Annals of Biomedical Engineering,* vol. 37, no. 11, pp. 2200-2217, Nov, 2009.

[8] A. K. Politis, G. P. Stavropoulos, M. N. Christolis *et al.*, "Numerical modeling of simulated blood flow in idealized composite arterial coronary grafts: Steady state simulations," *Journal Of Biomechanics,* vol. 40, no. 5, pp. 1125-1136, 2007.

[9] A. Valencia, and F. Baeza, "Numerical simulation of fluid-structure interaction in stenotic arteries considering two layer nonlinear anisotropic structural model," *International Communications In Heat And Mass Transfer,* vol. 36, no. 2, pp. 137-142, Feb, 2009.